

Bounds for the propagation speed of combustion flames

This article has been downloaded from IOPscience. Please scroll down to see the full text article.

2004 J. Phys. A: Math. Gen. 37 7185

(<http://iopscience.iop.org/0305-4470/37/29/002>)

View [the table of contents for this issue](#), or go to the [journal homepage](#) for more

Download details:

IP Address: 171.66.16.91

The article was downloaded on 02/06/2010 at 18:23

Please note that [terms and conditions apply](#).

Bounds for the propagation speed of combustion flames

Joaquim Fort¹, Daniel Campos², Josep R González³ and Joaquim Velayos³

¹ Departament de Física, Universitat de Girona, Campus de Montilivi, 17071 Girona, Catalonia, Spain

² Grup de Física Estadística, Departament de Física, Universitat Autònoma de Barcelona, E-08193 Bellaterra, Spain

³ Grup de Mecànica de Fluids, Departament d'Enginyeria Mecànica, Universitat de Girona, Campus de Montilivi, 17071 Girona, Catalonia, Spain

E-mail: joaquim.fort@udg.es, daniel.campos@uab.es, joseramon.gonzalez@udg.es and joaquim.velayos@udg.es

Received 23 February 2004, in final form 18 May 2004

Published 7 July 2004

Online at stacks.iop.org/JPhysA/37/7185

doi:10.1088/0305-4470/37/29/002

Abstract

We focus on a combustion model for premixed flames based on two coupled equations determining the spatial dynamics of temperature and fuel density. We rewrite these equations as a classical reaction-diffusion model, so that we can apply some known methods for the prediction of lower and upper bounds to the front speed. The predictions are compared to simulations, which show that our new bounds substantially improve those following from the linearization method, used in the previous work of Fort *et al* (2000 *J. Phys. A: Math. Gen.* **33** 6953). Radiative losses lead to pulses rather than fronts. We find a bound for their speed which (in contrast to the linearization one) correctly predicts the order of magnitude of the flame speed.

PACS numbers: 82.33.Vx, 02.60.Cb, 82.20.Nk, 82.40.–g

1. Introduction

The modelling of combustion processes is a recurrent item that has yielded a vast number of works during recent decades [1, 2]. As a consequence, this field has been divided into many different branches, every one is concerned about the study of a specific kind of situation. Nevertheless, because of the complexity of these chemical processes when one tries to deal with real systems, most authors have tended to build complicated methods which require large computer times, sometimes forgetting the analytical side of the models.

In this paper, we start from a simple model based on reaction-diffusion (RD) equations, a mathematical tool that has proved useful before in many systems involving front propagation, such as biological invasions [3], epidemics [4] and many others. RD approaches to combustion theory are also numerous [5–7]. Specifically, the model we illustrate here has been taken from the work by Warnatz *et al* [1]. We try to give a more analytical outlook to it, which allows us to study important parameters such as the front speed and the maximum temperature arising from the differential equations, and compare them to computer simulations.

Analytical expressions for the front speed v in RD equations are rarely achieved. Only for some simple reaction functions, such as the logistic growth [8] or the cubic nonlinearity [9], exact solutions are possible. For this reason, in section 2 we will work with different mathematical methods giving lower and upper bounds to the front speeds. Thus, our main objective lies in obtaining a theoretical range for the wavefront speed and observe if it agrees with the simulated results. It is also noteworthy because some previous analytical works [6, 7] have usually resorted to linearization methods in order to predict the flame speed. Here, we show by means of numerical simulations that linearization does not yield accurate results in RD approaches to combustion, and we provide some alternative techniques which substantially improve the predictions of the linearization approach. In section 3 we generalize the model to include radiation heat losses, which lead to pulse instead of front solutions. We find a bound for their speed which, in contrast to the linearization one, predicts speed with an order of magnitude that is consistent with that observed in the simulations. Section 4 is devoted to concluding remarks.

2. The front speed problem

The model we study here is restricted to the case of premixed flames (matter diffusion is not taken into account) in gases, rather than solid fuels (in the latter, the gas usually has a higher thermal diffusivity than the solid, which implies that the propagation direction of the flame does not necessarily coincide with the heat flux direction [10–13], so a one-dimensional model may be inappropriate). Heat convection is neglected, an approximation which is appropriate in some conditions (e.g., microgravity and free-fall experiments) and is a very useful first step before dealing with more complicated situations [14]. We first present the evolution equation for the temperature T of spherical flames in time t and radial space coordinate r . The rate of temperature change has a conductive term plus the reaction (combustion) term,

$$\rho_0 c \frac{\partial T}{\partial t} = \lambda \frac{\partial^2 T}{\partial r^2} + Q A \rho \left(e^{-\frac{E_a}{RT}} - e^{-\frac{E_a}{RT_0}} \right) \quad (1)$$

where ρ is the fuel density, T_0 is the environment temperature, c is the heat capacity, λ is the thermal conductivity and the combustion term follows the Arrhenius approximation [5], where Q is the heat produced by the combustion reaction per unit mass, R is the universal gas constant, E_a is the activation energy per mole and A is called the preexponential factor (its inverse is a characteristic reaction time). The second equation in our model is that of mass evolution,

$$\frac{\partial \rho}{\partial t} = -A \rho \left(e^{-\frac{E_a}{RT}} - e^{-\frac{E_a}{RT_0}} \right) \quad (2)$$

which accounts for the fuel consumption due to the chemical reactions, thus the same combustion term that has been introduced in (1). Equation (2) prevents our system from increasing its local temperature indefinitely (it may thus be regarded as a fuel-availability restriction). Thus, equation (2) is essential in order to obtain realistic solutions. According to it, the temperature will increase at each point of the system until the fuel becomes exhausted

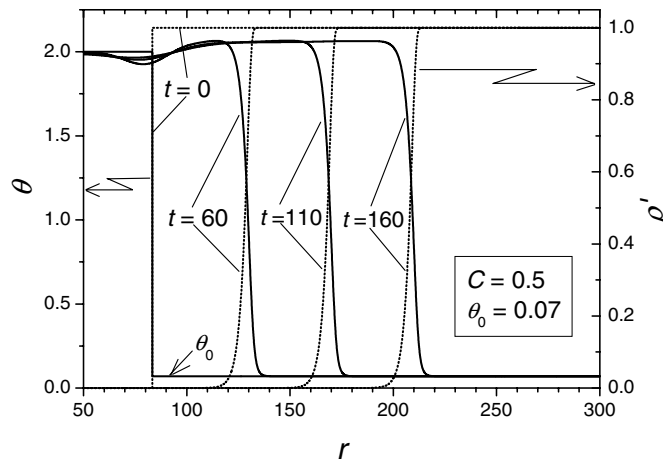


Figure 1. Examples of dimensionless temperature θ (full curves) and fuel density ρ' (dotted) profiles, obtained by means of computer simulations of equations (3) and (4), which do not take into account energy losses. The solutions are fronts (compare to the pulses in figure 4, where radiation losses are included).

and then it will remain constant, as no mechanisms of heat losses are considered here (they will be included in the following section). Thus, the solution expected in this section should have the form of a travelling front (see, e.g., figure 1).

It is important to note in equations (1) and (2) that we have added a combustion term (the last one in the right-hand side) in which the room temperature T_0 appears. This extra term serves us to let the initial state $T = T_0$ be a steady state (otherwise, we would not be able to apply some analytical methods which will be very useful, as shown below). Therefore, although we do not include in these equations heat losses explicitly, we apply the usual so-called ‘cold boundary layer’ heat loss (and reaction cut-off) term ensuring steadiness for the initial state, i.e. the very reasonable result $\partial T/\partial t = 0$ (and $\partial \rho/\partial t = 0$) from equations (1), (2) for the case in which all points of the system are at room temperature, $T = T_0$. Note that at high temperatures $\rho_0 e^{-\frac{E_a}{RT_0}} \ll \rho e^{-\frac{E_a}{RT}}$ and $\rho e^{-\frac{E_a}{RT_0}} \ll \rho e^{-\frac{E_a}{RT}}$, so that we have for the cold-boundary term $\rho e^{-\frac{E_a}{RT}} - \rho_0 e^{-\frac{E_a}{RT_0}} \simeq \rho(e^{-\frac{E_a}{RT}} - e^{-\frac{E_a}{RT_0}})$, as done in our equations (1), (2) and usual in the combustion literature [5]. We mention that we have checked the validity of this approximation explicitly, by means of numerical simulations with reasonable values of the parameters and comparing the results to simulations without using this approximation. Our numerical integrations assume an initial step function for the temperature and fuel density (with $T(r, t = 0) = T_0$ for those values of r such that $\rho(r, t = 0) = \rho_0$, see, e.g., figure 1).

Now, we rewrite for convenience equations (1) and (2) in the dimensionless form

$$\frac{\partial \theta}{\partial t'} = \frac{\partial^2 \theta}{\partial r'^2} + \rho'(e^{-\frac{1}{\theta}} - e^{-\frac{1}{\theta_0}}) \tag{3}$$

$$\frac{\partial \rho'}{\partial t'} = -C\rho'(e^{-\frac{1}{\theta}} - e^{-\frac{1}{\theta_0}}) \tag{4}$$

where we have defined the new dimensionless variables and parameters

$$\theta \equiv T \frac{R}{E_a} \tag{5}$$

$$t' \equiv t \frac{RQA}{cE_a} \quad (6)$$

$$r' \equiv r \sqrt{\frac{RQA\rho_0}{\lambda E_a}} \quad (7)$$

$$\rho' \equiv \frac{\rho}{\rho_0} \quad (8)$$

$$C \equiv \frac{cE_a}{RQ}. \quad (9)$$

We will look for an expression for the maximum temperature. An easy way to do so is by integrating (3) and (4) from $t' = 0$ to $t' = \infty$. By doing this and introducing the boundary conditions

$$\begin{aligned} \theta(t' = \infty) &= \theta_{\max} & \theta(t' = 0) &= \theta_0 \\ \rho'(t' = \infty) &= 0 & \rho'(t' = 0) &= 1 \end{aligned} \quad (10)$$

we finally find the expression

$$\theta_{\max} = \theta_0 + \frac{1}{C} \quad (11)$$

or, in terms of the original variable T ,

$$T_{\max} = T_0 + \frac{Q}{c}. \quad (12)$$

In the derivation of equation (11) we have assumed that the thermal gradient is non-zero only in a narrow region (which determines the position of the flame front). For this reason, we have considered that the thermal conduction term, when integrated over all times from 0 to ∞ , is negligible. In order to prove the validity of our assumption, we can observe that equation (12) is just a special case of the Zeldovich equation for the conservation of energy [5]

$$\rho_0 c(T - T_0) = Q(\rho_0 - \rho) \quad (13)$$

or

$$\theta - \theta_0 = \frac{1 - \rho'}{C} \quad (14)$$

in the limit where t goes to infinity (so $T \rightarrow T_{\max}$ and $\rho \rightarrow 0$). A comparison between the prediction in (11) and simulations from our general equations is given in figure 2, where the agreement found for different values of C and θ_0 is excellent. This confirms the validity of equation (11).

By means of equation (13), we can rewrite equation (3) getting rid of the field ρ' ,

$$\frac{\partial \theta}{\partial t'} = \frac{\partial^2 \theta}{\partial r'^2} + [1 - C(\theta - \theta_0)](e^{-\frac{1}{\theta}} - e^{-\frac{1}{\theta_0}}) \quad (15)$$

which using equation (11) becomes

$$\frac{\partial \theta'}{\partial t'} = \frac{\partial^2 \theta'}{\partial r'^2} + C(1 - \theta')\left(e^{-\frac{1}{\theta_0 + (\theta_{\max} - \theta_0)\theta'}} - e^{-\frac{1}{\theta_0}}\right) \quad (16)$$

where we have introduced the new dimensionless variable

$$\theta' \equiv \frac{\theta - \theta_0}{\theta_{\max} - \theta_0}. \quad (17)$$

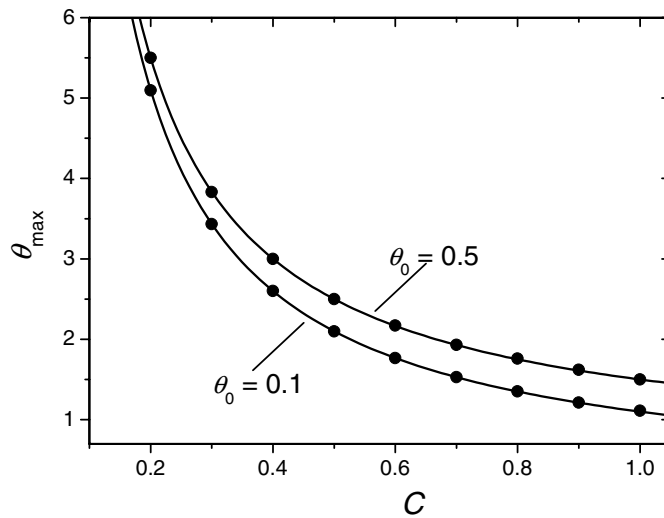


Figure 2. Theoretical values (curves) and observed in numerical simulations of equations (3), (4) (circles) for θ_{\max} as a function of the fuel parameter C and for different values of θ_0 .

The main advantage of this new expression lies in the fact that we have managed to achieve an RD equation in terms of just one variable (as (16) is not coupled to the density ρ') which moreover varies in the interval $0 < \theta' < 1$, with both extremes $\theta' = 0$ (room temperature $T = T_0$) and $\theta' = 1$ (maximum flame temperature $T = T_{\max}$) being steady states (i.e., such that the last term in equation (16) vanishes). This framework corresponds precisely to that of the theory of dimensionless RD equations, which have the general form

$$\frac{\partial n}{\partial t'} = \frac{\partial^2 n}{\partial r'^2} + F(n) \tag{18}$$

and have been widely employed in mathematical works for predicting bounds for the speed of fronts [15–19], so now we will be able to apply such methods straight. In the following, we will present four of these methods taken from the literature and will obtain the bounds predicted by them.

2.1. Kolmogorov–Petrovski–Piskunov (KPP) method

This method [15] is based on the linearization of the partial differential equation after introducing the variable $z = r' - vt'$ (where v is the dimensionless velocity). Requiring the solution to die out exponentially for $z \rightarrow \infty$, one finds that the speed v must accomplish the well-known condition

$$v \geq v_{\text{KPP}} = 2 \sqrt{\left(\frac{dF}{dn}\right)_{n=0}} \tag{19}$$

so a lower bound for v arises.

For the specific case we are considering, the condition turns into

$$v \geq v_{\text{KPP}} = 2 \frac{e^{-\frac{1}{2\theta_0}}}{\theta_0} \tag{20}$$

where the relation in (11) has been used. Before comparing to numerical simulations, we discuss other interesting methods.

2.2. Zeldovich–Frank–Kamenetski (ZFK) method

In this approach, the assumption is made that near the chemical reaction zone (which also determines the position of the front), the thermal gradient is large. Thus in the reaction zone, the heat conduction term is presumably very large and dominates over the temporal derivative at the left in (1) (which can then be neglected) and so that equation becomes ordinary [5, 16],

$$0 \leq \lambda \frac{\partial^2 T}{\partial r^2} + Q A \rho \left(e^{-\frac{E_a}{RT}} - e^{-\frac{E_a}{RT_0}} \right). \quad (21)$$

Integrating this equation in the variable $q \equiv \lambda \frac{\partial T}{\partial r}$ and taking into account that the heat flux q (energy per unit area and time) must equal the energy released by combustion in the reaction zone as the flame propagates, i.e. that the relation

$$\lambda \frac{\partial T}{\partial r} = Q \rho_0 v \quad (22)$$

holds (for the full detail, see [5, 16]), one arrives in our case to the final expression

$$v \geq v_{\text{ZFK}} = \sqrt{2 \int_0^1 d\theta' C(1 - \theta') \left(e^{-\frac{1}{\theta_0 + (\theta_{\text{max}} - \theta_0)\theta'}} - e^{-\frac{1}{\theta_0}} \right)}. \quad (23)$$

For the more general dimensionless equation (18), the corresponding result is obviously

$$v \geq v_{\text{ZFK}} = \sqrt{2 \int_0^1 F(n) dn}. \quad (24)$$

We note that for this method the analytic expression found, equation (23), is not possible to solve explicitly, but implicit integration methods lead us to a solution easily.

2.3. Benguria–Depassier (BD) method

This method is based on variational principles. The mathematical details of this development can be found in [17]. According to that work, an approximate lower bound for equation (18) is

$$v \geq v_{\text{BDI}} = \frac{4\sqrt{n} \left(\int_0^1 F(n) dn \right)^{n+\frac{1}{2}}}{\left(\int_0^1 n F(n) dn \right)^n} \quad (25)$$

where n is an arbitrary value between the interval $0.5 < n < 1$ (so we will analyse here the two limit cases $n = 0.5$ and $n = 1$). The same variational method also allows us to obtain upper bounds to the speed of front solutions to the differential equation; a good example is the expression found in [18],

$$v \leq v_{\text{BDu}} = 2 \sqrt{\sup \left[\frac{dF(n)}{dn} \right]}. \quad (26)$$

The application of these bounds to the model we propose here leads us to

$$v \geq v_{\text{BDI}} = \frac{4\sqrt{n} \left(\int_0^1 d\theta' C(1 - \theta') \left(e^{-\frac{1}{\theta_0 + (\theta_{\text{max}} - \theta_0)\theta'}} - e^{-\frac{1}{\theta_0}} \right) \right)^{n+\frac{1}{2}}}{\left(\int_0^1 d\theta' \theta' C(1 - \theta') \left(e^{-\frac{1}{\theta_0 + (\theta_{\text{max}} - \theta_0)\theta'}} - e^{-\frac{1}{\theta_0}} \right) \right)^n} \quad (27)$$

$$v \leq v_{\text{BDu}} = 2 \sqrt{\sup \left[-C \left(e^{-\frac{1}{\theta_0 + (\theta_{\text{max}} - \theta_0)\theta'}} - e^{-\frac{1}{\theta_0}} \right) + \frac{C(1 - \theta')(\theta_{\text{max}} - \theta_0)}{(\theta_0 - (\theta_{\text{max}} - \theta_0)\theta')^2} e^{-\frac{1}{\theta_0 + (\theta_{\text{max}} - \theta_0)\theta'}} \right]} \quad (28)$$

where the same kind of integrals as those in the ZFK method appear, so implicit methods are required for obtaining the exact solution.

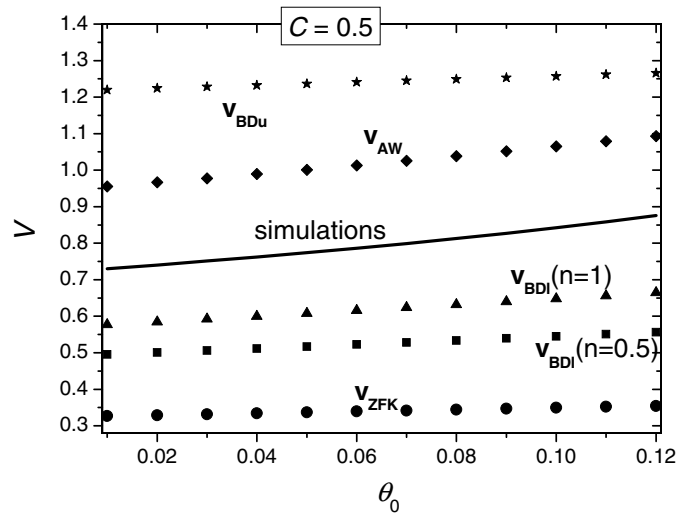


Figure 3. Comparison between all the bounds predicted (symbols) and the exact value of v from simulations (curve) of the general equations (3), (4), which do not take energy losses into account. Lower bounds plotted are those from BD (squares for $n = 0.5$ and triangles for $n = 1$) and ZFK (circles). The upper bounds correspond to BD (rhombus) and AW (stars). We have used $C = 0.5$.

2.4. Aronson–Weinberger (AW) method

This method uses mathematical analysis [19] to derive a new upper bound for equation (18), given by

$$v \leq v_{AW} = 2 \sqrt{\sup \left[\frac{F(n)}{n} \right]}. \tag{29}$$

Application of this expression to our equation (16) allows us to write finally

$$v \leq v_{AW} = 2 \sqrt{\sup \left[C \frac{1 - \theta'}{\theta'} \left(e^{-\frac{1}{\theta_0 + (\theta_{max} - \theta_0)\theta'}} - e^{-\frac{1}{\theta_0}} \right) \right]}. \tag{30}$$

Now we have four different methods, which provide us with six lower and upper bounds that will constrain the value of the front speed v . Thus we can perform a comparison between these bounds and the speed of fronts arising from simulations of the general equations (3), (4). Figure 3 summarizes the results found and allows us to reach the following conclusions:

- (i) All the lower (upper) bounds reported lead us really to velocities which are below (above) those from the simulations, so all the former methods seem suitable to tackle the problem we are interested in.
- (ii) The better fits to the simulated speed are the lower bound by the BD method (with $n = 1$) and the upper bound by AW. It improves the results obtained by BD in [17].
- (iii) An additional conclusion comes from the study of the KPP case. The lower bound corresponding to this method does not appear in figure 3 because the values found from its result (20) are far below the other predictions (two or three orders of magnitude below). Paradoxically, this method is the most widely used for obtaining the front speed in general RD models such as (18), because of its simplicity and the good results obtained for some specific cases (e.g., the logistic growth) for which the KPP bound for v coincides with the exact solution [20]. In consequence, our work proves that the KPP linearization is not

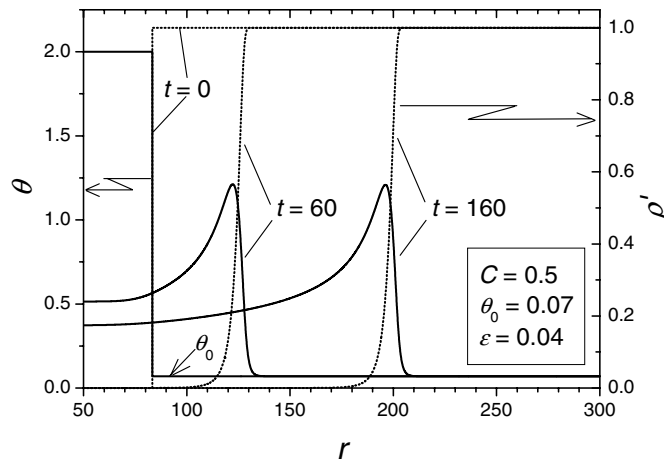


Figure 4. Examples of dimensionless temperature θ (full curves) and fuel density ρ' (dotted) profiles, obtained by means of computer simulations of equations (32) and (33), which take into account radiative energy losses. The solutions are pulses (compare these profiles to those in figure 1, which have a front shape and are faster because radiation losses are not included in figure 1).

a suitable approximation for growth terms in the Arrhenius form. Thus, we claim that some previous works that have focused on this possibility (see, for example, [6, 7]) need to be revised, as follows. In this section we have offered some alternative methods for the evaluation of the propagation speed that clearly improve the KPP predictions and lead to the correct order of magnitude and a finite range for v , as shown in figure 3.

We stress that equation (11) for the maximum temperature is essential as it has allowed us to perform a theoretical analysis of the model: otherwise, we cannot find an explicit expression for θ_{\max} and so the main variable $0 < \theta' < 1$ cannot be defined properly and most of the methods applied above break down. On the other hand, the more general equation (13) is essential in order to reduce a two-variable system (equations (1), (2)) into a single one (equation (16)), which is absolutely necessary in most of the methods applied above.

3. The pulse speed problem: radiation losses

Up to this point we have considered, following other authors [17], the case without energy losses⁴. This is of course absolutely unrealistic because real flames do extinguish. But is extremely useful before attempting a qualitatively realistic description. Such an improved description is precisely the aim of this section. In other words, now the flame cools down after the fuel is exhausted. This is why instead of *fronts* (figure 1) we obtain *pulse* solutions (figure 4). Mathematically, instead of equation (1) we now consider

$$\rho_0 c \frac{\partial T}{\partial t} = \lambda \frac{\partial^2 T}{\partial r^2} + Q A \rho \left(e^{-\frac{E_a}{RT}} - e^{-\frac{E_a}{RT_0}} \right) - 4a\sigma(T^4 - T_0^4) \quad (31)$$

which is nothing but equation (1) with an additional term which take cares of radiative heat losses, and has the usual form [21–23, 6]. Here a is the absorption coefficient and σ is the

⁴ It may also be noted that our detailed derivation of equation (16) shows that the source term, namely $C(1 - \theta') \left(e^{-\frac{1}{\theta_0 + (\theta_{\max} - \theta_0)\theta'}} - e^{-\frac{1}{\theta_0}} \right)$, is different from equation (2) in [17]. A major difference between our section 2 and [17] is that we have considered the AW speed, which was not taken into account in [17], and we have shown that it is the best upper bound to the speed in the problem considered.

Stefan–Boltzmann constant. Equation (2) of course still holds and, proceeding as above, we arrive at

$$\frac{\partial \theta}{\partial t'} = \frac{\partial^2 \theta}{\partial r'^2} + \rho' (e^{-\frac{1}{\theta}} - e^{-\frac{1}{\theta_0}}) - \varepsilon (\theta^4 - \theta_0^4) \tag{32}$$

$$\frac{\partial \rho'}{\partial t'} = -C \rho' (e^{-\frac{1}{\theta}} - e^{-\frac{1}{\theta_0}}) \tag{33}$$

which replace equations (3), (4). We have defined

$$\varepsilon \equiv \frac{4a\sigma}{QA\rho_0\left(\frac{E_a}{R}\right)} \tag{34}$$

which may be called the dimensionless emissivity.

As mentioned above, the main point now is that heat losses will extinguish the flame. Thus, the first of the boundary conditions (10) no longer corresponds to the maximum flame temperature but to the room temperature,

$$\begin{aligned} \theta(t' = \infty) &= \theta_0 & \theta(t' = 0) &= \theta_0 \\ \rho'(t' = \infty) &= 0 & \rho'(t' = 0) &= 1. \end{aligned} \tag{35}$$

Integrating equation (32) from $t' = 0$ to ∞ , we obtain instead of equation (11)

$$\frac{1}{C} = \varepsilon \int_0^\infty dt' (\theta^4 - \theta_0^4) \tag{36}$$

which has a very simple physical interpretation: the dimensionless reaction heat $1/C$ transforms into radiation energy (in contrast to equation (11), which means that in the toy model of section 2, the reaction heat transformed into a net temperature increase).

Integrating equation (33) from $t' = 0$ until t' we obtain

$$\rho' - 1 = -C \int_0^{t'} dt' \rho' (e^{-\frac{1}{\theta}} - e^{-\frac{1}{\theta_0}}) \tag{37}$$

which used in equation (32) —also integrated from $t' = 0$ until t' —yields

$$\theta - \theta_0 = \frac{1 - \rho'}{C} - \int_0^{t'} dt' \varepsilon (\theta^4 - \theta_0^4) \tag{38}$$

which generalizes equation (14). From this we can find an expression for ρ' and use it in (32), so as to get rid of the field ρ' . This yields

$$\frac{\partial \theta}{\partial t'} = \frac{\partial^2 \theta}{\partial r'^2} + \left[1 - C(\theta - \theta_0) - C \int_0^{t'} dt' \varepsilon (\theta^4 - \theta_0^4) \right] (e^{-\frac{1}{\theta}} - e^{-\frac{1}{\theta_0}}) - \varepsilon (\theta^4 - \theta_0^4). \tag{39}$$

Finally we may make use of equation (36) and obtain

$$\frac{\partial \theta}{\partial t'} = \frac{\partial^2 \theta}{\partial r'^2} + \left[1 - C(\theta - \theta_0) - \frac{\int_0^{t'} dt' (\theta^4 - \theta_0^4)}{\int_0^\infty dt' (\theta^4 - \theta_0^4)} \right] (e^{-\frac{1}{\theta}} - e^{-\frac{1}{\theta_0}}) - \varepsilon (\theta^4 - \theta_0^4) \tag{40}$$

which generalizes equation (15). There are two new terms: the last one, and the quotient of integrals inside the square bracket.

3.1. Kolmogorov–Petrovski–Piskunov method

The quotient of integrals inside the square bracket in equation (39) obviously tends to zero in the leading edge of the pulse ($\theta = \theta_0 + \delta$, with $\delta \ll \theta_0$). Therefore, the linearization method may be applied neglecting this term, and in the front frame equation (40) becomes in first order (we define $z \equiv r' - vt'$)

$$-v \frac{d\delta}{dz} = \frac{d^2\delta}{dz^2} + \frac{e^{-\frac{1}{\theta_0}}}{\theta_0^2} \delta - 4\varepsilon\theta_0^4 \delta.$$

As usual in the linearization method, we look for a solution which dies out as $\delta \sim \exp[-\lambda z]$. Using this and requiring that $\lambda > 0$ we find the lower bound

$$v \geq v_{\text{KPP}} = 2 \sqrt{\frac{e^{-\frac{1}{\theta_0}}}{\theta_0^2} - 4\varepsilon\theta_0^4} \quad (41)$$

which reduces to equation (20) for $\varepsilon = 0$, as it should. In fact, equation (41) was derived previously (equation (8) in [6]) in a different context ([6] did not take into account the fuel-availability restriction (2)). As in the previous (i.e., non-radiative) section, our main point, however, is not to compare the model we use here to that in [6], but to show that the KPP method (which was the only one applied in [6]) gives much worse predictions than one or several of the following methods, which were not considered in [6].

3.2. Zeldovich–Frank–Kamenetski method

Equation (40) is clearly much more complicated than (16) and we see no way to generalize the approach in section 3.2) to derive a similar result for the case of radiation losses.

3.3. Aronson–Weinberger (AW) method

This approach can indeed be applied to *pulse* in addition to *front* solutions. This is simply because in [19], equation (4.2), the authors assume that $\theta' \rightarrow 0$ as $r' - vt' \rightarrow +\infty$, with $v > 0$ the speed of the (pulse or front) wave, but no assumption is made for the limit $r' - vt' \rightarrow +\infty$ (in which $\theta' \rightarrow 1$ corresponds to front and $\theta' \rightarrow 0$ to a pulse). This is also explicitly stressed at many places in the very interesting paper [24], which outlines the same proof as the better-known [19].

First of all, we note that the integrals in equation (40) are always positive. Thus, they will yield a lower effective heat reaction term (and thus, obviously a lower flame speed) than that of equation (40) if those integrals are neglected, namely

$$\frac{\partial\theta}{\partial t'} = \frac{\partial^2\theta}{\partial r'^2} + [1 - C(\theta - \theta_0)](e^{-\frac{1}{\theta}} - e^{-\frac{1}{\theta_0}}) - \varepsilon(\theta^4 - \theta_0^4). \quad (42)$$

In other words, this equation may be used together with the AW method to yield an upper bound for the speed. In order to do so, one more step is necessary since the AW method holds only for equations of the form

$$\frac{\partial n}{\partial t'} = \frac{\partial^2 n}{\partial r'^2} + F(n) \quad (43)$$

with $F(0) = F(1) = 0$ and as long as that all possible values of the field n are between both limits (i.e., $0 \leq n \leq 1$, the bound $n = 1$ being reached for fronts but not for pulses in general, since for pulses both the initial and the final local states are $n = 0$). Equation (42) does not satisfy these conditions. But the same happened for equation (15)

and, indeed, this is why in the former section we defined θ' by means of equation (17), and made use of equation (11) to derive (16). Equation (11) now does not apply (instead, equation (36) holds, as explained above). Therefore, we no longer make use of θ' . Instead of using $\theta_{\max} = \theta_0 + \frac{1}{C}$, as in equation (11), which was nothing but a root to the source term in (15), i.e. $[1 - C(\theta_{\max} - \theta_0)](e^{-\frac{1}{\theta^*}} - e^{-\frac{1}{\theta_0}}) = 0$, let us analogously define θ^* such that it is a root to the source term in (42), i.e.

$$[1 - C(\theta^* - \theta_0)](e^{-\frac{1}{\theta^*}} - e^{-\frac{1}{\theta_0}}) - \varepsilon(\theta^{*4} - \theta_0^4) = 0 \tag{44}$$

(we have found, in the examples below, that it is very simple to find the appropriate root in practice: one just has to use numerical methods beginning with a low value of ε and looking for a root near the corresponding one for $\varepsilon = 0$, i.e. $\theta_0 + \frac{1}{C}$).

We also introduce the new variable

$$\theta'' \equiv \frac{\theta - \theta_0}{\theta^* - \theta_0} \tag{45}$$

which plays the same role as equation (17) in the former section. Indeed, in terms of this new variable equation (42) becomes

$$\frac{\partial \theta''}{\partial t'} = \frac{\partial^2 \theta''}{\partial r'^2} + F(\theta'') \tag{46}$$

with

$$F(\theta'') = \frac{1 - C(\theta^* - \theta_0)\theta''}{\theta^* - \theta_0} (e^{-\frac{1}{\theta_0 + (\theta^* - \theta_0)\theta''}} - e^{-\frac{1}{\theta_0}}) - \varepsilon \frac{(\theta_0 + (\theta^* - \theta_0)\theta'')^4 - \theta_0^4}{\theta^* - \theta_0} \tag{47}$$

which satisfies that $F(0) = F(1) = 0$, as desired and in complete analogy with equation (16) in the previous section. Thus we may now finally apply the AW upper bound for the speed (29), which yields

$$v \leq v_{AW} = 2\sqrt{\sup \left[\left(\frac{1}{(\theta^* - \theta_0)\theta''} - C \right) (e^{-\frac{1}{\theta_0 + (\theta^* - \theta_0)\theta''}} - e^{-\frac{1}{\theta_0}}) - \varepsilon \frac{(\theta_0 + (\theta^* - \theta_0)\theta'')^4 - \theta_0^4}{(\theta^* - \theta_0)\theta''} \right]}. \tag{48}$$

This result is specially rewarding if we note that in the case considered in the former section, the AW speed is the best upper bound and moreover gives the correct order of magnitude for the speed. Numerical simulations have allowed us to see this in the previous section for the front (or no radiation) case (figure 3). Figure 5 shows that the same happens for the pulse (or radiation) case, which predicts extinguishment, in contrast to the case of the previous section and [17]. On the other hand, the KPP result (41) is several orders of magnitude below the results from the simulations (this is why it does not appear in figure 5), as it already happened in the previous section. We conclude that the AW method, in contrast to the other ones, can be applied to the case of heat losses, and it provides an upper bound that correctly constrains the flame speed. In figure 5, it may also be observed that the AW result correctly predicts the speed, as far as its order of magnitude is concerned.

3.4. Benguria–Depassier (BD) method

Equation (40) is clearly not of the form (18), so that the BD method cannot be applied to derive lower bounds. One may want to neglect the integrals and try to derive an upper bound, as we have done for the AW method above. However, it is not clear whether the BD method, which was devised to deal with fronts [17], can be modified to deal with pulses. In any case, we know from the non-radiative case (figure 3) that the AW yields a better bound, so it is not our aim here to enquire this point in further detail.

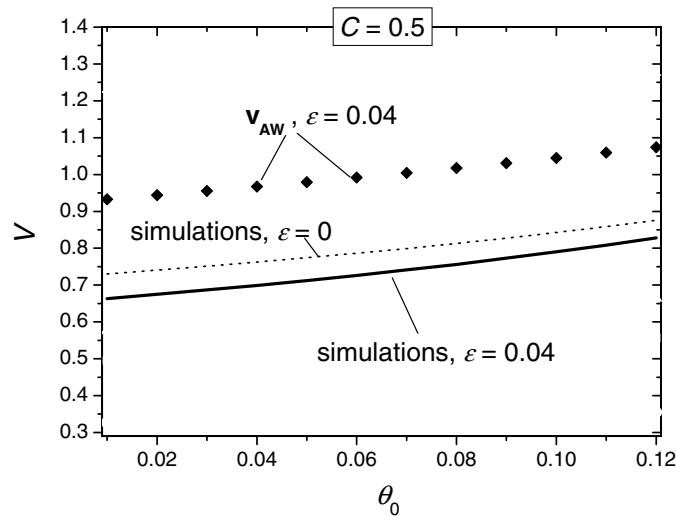


Figure 5. AW bound for pulse solutions (rhombus) versus simulations (full curve). In contrast to the single other applicable method (namely, the linearization one), the AW approach correctly predicts the order of magnitude of the flame speed. For comparison we also include, as a dotted curve, the results from the simulations of fronts (from figure 3), rather than pulses. It is seen then that pulses are slower, as it was to be expected intuitively, since they correspond to a lower flame energy (because of radiative heat losses).

4. Concluding remarks

The analytical study of combustion models is of great interest for prediction purposes. Nevertheless, one finds that, in practice, some assumptions must be made in order to achieve explicit expressions from such models. In this paper, we have illustrated a case which has been proposed before by Warnatz *et al* [1] for the modelization of premixed laminar flames in a gaseous fuel. From equation (13) for the conservation of the energy, we have found that the evolution of the temperature can be put in the form of a single dimensionless RD equation (equation (16)).

Without taking into account heat losses (section 2), reduction to a single RD equation has allowed us to apply different mathematical methods proposed before for obtaining different lower and upper bounds to the speed v of the travelling front solutions arising from this type of equation. Four different mathematical methods have been reported and the outcoming expressions have been compared to simulations. The results (in figure 3) confirm that the four methods are compatible with the general equation (16) proposed in this case. Moreover, comparing them to the predictions has led us to conclude that the BD and the AW methods are those which better fit the speed obtained from simulations. This is in sharp contrast to the KPP method, which has been used before [6, 7], but is not a good approximation for Arrhenius-like reaction terms (specifically, we find that the lower bound predicted is two orders of magnitude below the simulation results).

When heat losses are included (section 3), we obtain pulse waves (figure 4) rather than wavefronts (figure 1), the single RD equation (16) generalizes into an integro-differential equation (equation (40)), and most of the known analytic methods break down because of mathematical complications. But we have shown that the AW approach can even then be

applied, it yields a useful bound for the speed and correctly predicts its order of magnitude (figure 5).

Before closing, we would like to stress that we have assumed here that there is no velocity field (i.e., we have dealt with the non-advective case). In most practical situations, this is realistic if convective effects can be neglected (some such important examples are microgravity environments and free-fall experiments [14, 25]). The other case, namely that of a non-homogeneous fluid velocity field, is more realistic in numerous important cases [26] and obviously more complicated mathematically [27] (some such important open problems deal with flame quenching—i.e., propagation failure due to, e.g., heat losses—[28] and with the dependence of the front speed with the features of the velocity fields [29, 30]). Then, our approach is not straightforward to apply, but some interesting alternatives are singular perturbation analysis, Hamilton–Jacobi dynamics and the local-equilibrium approach. These three methods have been recently proved very useful in other instances of front solutions to non-homogeneous fields in reaction-diffusion equations [31, 32].

Finally, it is worth noting that also in the non-advective case there are subtle behaviours beyond those considered here, e.g. the effect of sufficiently smooth initial conditions on the front speed [33]. In this case, a very powerful technique that has only very recently begun to be applied is based on Hamilton–Jacobi dynamics [34]. These topics lie out of the scope of this paper but deserve further attention.

Acknowledgments

We thank Joan Ruiz for some independent runs of our simulation programs. Daniel Campos acknowledges the Departament d'Universitats, Recerca i Societat de la Informació of the Generalitat de Catalunya. Partially funded by the Generalitat de Catalunya under grant SGR-2001-00186, and by the MICYT under grant REN-2003-00185 CLI.

References

- [1] Warnatz U, Maas U and Dibble R W 2001 *Combustion* (Berlin: Springer)
- [2] Linan A and Williams F A 1993 *Fundamental Aspects of Combustion* (New York: Oxford University Press)
- [3] Shigesada N and Kawasaki K 1997 *Biological Invasions: Theory and Practice* (New York: Oxford University Press)
- [4] Méndez V 1998 *Phys. Rev. E* **57** 3622
- [5] Zeldovich Ya B, Barenblatt G I, Librovich V B and Makhviladze G M 1985 *The Mathematical Theory of Combustion and Explosions* (New York: Consultants Bureau)
- [6] Fort J, Pujol T and Cukrowski A S 2000 *J. Phys. A: Math. Gen.* **33** 6953
- [7] Weber R O 1991 *Int. J. Wildland Fire* **1** 245
- [8] Fisher R A 1937 *Ann. Eugenics* **7** 355
- [9] Ben-Jacob E *et al* 1985 *Physica D* **14** 348
- [10] De Ris J N 1969 *12th Int. Symp. on Combustion* (Pittsburg: The Combustion Institute) p 241
- [11] Williams F A 1977 *16th Int. Symp. on Combustion* (Pittsburg: The Combustion Institute) p 1281
- [12] Delichatsios M A 1986 *Combust. Sci. Technol.* **44** 257
- [13] Ronney P D *et al* 1995 *Combust. Flame* **100** 474
- [14] Ronney P D 1998 *27th Int. Symp. on Combustion* (Pittsburg: The Combustion Institute) p 2485
- [15] Kolmogorov A, Petrovski I and Piskunov N 1937 *Bull. Univ. Moscow, Ser. Int. A* **1** 1
- [16] Zeldovich Y B and Frank-Kamenetzki D A 1938 *Acta Physicochim. USSR* **9** 341
- [17] Benguria R D, Cisternas J and Depassier M C 1995 *Phys. Rev. E* **52** 4410
- [18] Benguria R D and Depassier M C 1998 *Phys. Rev. E* **57** 6493
- [19] Aronson D G and Weinberger H F 1978 *Adv. Math.* **30** 33
- [20] Benguria R D and Depassier M C 1994 *Phys. Rev. Lett.* **73** 2272
- [21] Joulin G and Clavin P 1976 *Acta Astronaut.* **3** 223

-
- [22] Joulin G and Clavin P 1979 *Combust. Flame* **35** 139
 - [23] Williams F A 1985 *Combustion Theory* (Reading: Perseus), specially pp 646 and 279
 - [24] Aronson D G and Weinberger H F 1975 *Partial Differential Equations and their Applications* (Berlin: Springer) p 5
 - [25] Ronney P D 1998 *Combust. Sci. Technol.* **59** 123
 - [26] Peters N 2000 *Turbulent Combustion* (Cambridge: Cambridge University Press)
 - [27] Xin J 2000 *SIAM Rev.* **42** 161
 - [28] Buckmaster J 1976 *Combust. Flame* **26** 151
 - [29] Constantin P, Kiselev A, Oberman A and Ryzhik L 2000 *Arch. Ration. Mech. Anal.* **154** 53
 - [30] Abel M, Celani A, Vergni D and Vulpiani A 2001 *Phys. Rev. E* **64** 046307
 - [31] Méndez V, Fort J, Rotstein H and Fedotov S 2003 *Phys. Rev. E* **78** 041105
 - [32] Mendez V, Campos D and Fort J 2004 *Phys. Rev. E* **69** 016613
 - [33] Ebert U and van Saarloos W 2000 *Physica D* **146** 1
 - [34] Méndez V, Fort J and Pujol T 2003 *Phys. Rev. E* **67** 016213